

## SYNTHESIS AND PROPERTIES OF INORGANIC COMPOUNDS

# Complex Antimony(III) Oxohalides: Synthesis and Physicochemical Properties

A. E. Panasenko, L. A. Zemnukhova, V. Ya. Kavun, and E. B. Merkulov

Institute of Chemistry, Far East Branch, Russian Academy of Sciences, Vladivostok, Russia

e-mail: panasenko@ich.dvo.ru

Received June 15, 2010

**Abstract**—Complexes of the formula  $MSb_2BrF_4O$  ( $M = K, Rb,$  and  $NH_4$ ) were obtained from aqueous solutions of  $SbF_3$  and  $MBr$  and examined by chemical analysis, X-ray diffraction, thermal analysis, and IR, Raman, and  $^{19}F$  NMR spectroscopy. It was found that the red reflectance is 74–97% and the UV reflectance is 7–15%. The highest averaged reflectance (93%) was observed for  $KSb_2BrF_4O$ . The decomposition temperatures of  $MSb_2BrF_4O$  ( $M = K, Rb,$  and  $NH_4$ ) are 230, 197, and 223°C, respectively.

**DOI:** 10.1134/S0036023612020192

Many antimony(III) compounds have found wide practical use:  $Sb_2O_3$ ,  $SbOHal$ ,  $Sb_4O_5Hal_2$ , and  $Sb_8O_{11}Hal_2$  ( $Hal = Cl$  and  $Br$ ) are employed as fireproofing agents, pigments, and polymer and dye fillers;  $SbF_3$  is used in metallurgy and textile industry;  $KSbF_4$  is a good ionic conductor [1]. In aqueous solutions, antimony(III) compounds undergo hydrolysis. It is known [2, 3] that the systems  $MHal-SbF_3-H_2O$  ( $M = K, Rb,$  and  $Cs$ ;  $Hal = Cl, Br,$  and  $I$ ) produce the complex oxohalides  $MSb_2HalF_4O$ . The literature data on the properties of these complexes are desultory.

The goal of this study was to determine the conditions for the formation of the complexes  $MSb_2BrF_4O$  ( $M = K, Rb,$  and  $NH_4$ ) and examine their structures, morphology, optical properties, thermal behavior, and ionic mobility. These studies were carried out in comparison with the known homoleptic fluoride analogs  $MSb_2F_7$  and simple antimony oxohalides such as  $SbOCl$ ,  $Sb_4O_5Cl_2$ ,  $Sb_3O_2F_5$ , and  $Sb_8O_{11}Br_2$ .

### EXPERIMENTAL

The complex oxohalides  $MSb_2BrF_4O$  ( $M = K, Rb,$  and  $NH_4$ ) were prepared by mixing a solution of  $KBr$ ,  $RbBr$ , or  $NH_4Br$  with a solution of  $SbF_3$  in a ratio of 0.4–3 : 1, 1 : 1, or 0.75–3 : 1, respectively [4]. Simple

oxohalides and complex fluoroantimonates(III) were obtained as described in [4, 5].

The compounds obtained were examined by chemical analysis, X-ray powder diffraction, IR spectroscopy, and thermal analysis. The contents of  $Br, F, N,$   $Rb,$  and  $Sb$  were determined using chemical analysis and spectrometry (in the case of  $K$ , by spectrometry alone). The chemical analytic techniques included bromatometric titration (for  $Sb$ ), the procedure described in [6] (for  $F$ ), the Volhard method [7] (for  $Br$ ), and the Kjeldahl method [8] (for  $N$  in the form of  $NH_4^+$  cations). Spectrometric analysis of complex antimony(III) oxohalides was performed by inductively coupled plasma atomic emission spectroscopy (ICP AES) on a Plasmaquant 110 spectrophotometer. Elemental analysis data are given in Table 1.

X-ray diffraction patterns were recorded on a Bruker D8 ADVANCE X-ray diffractometer ( $CuK_\alpha$  radiation). The patterns were identified against the PDF-2 powder diffraction file with the EVA program. IR spectra were recorded on a Shimadzu Prestige-21 FTIR spectrometer in the 400–4000  $cm^{-1}$  range. Raman spectra were recorded on a TriVista Raman spectrometer. Diffuse reflection spectra were recorded on a Hitachi U-3010 spectrophotometer in the 190–900 nm

**Table 1.** Elemental analysis data for the oxohalides  $M_pSb_kO_mHal_n$

Compound	Contents of the elements, %*			
	M	Sb	Br	F
$KSb_2BrF_4O$	8.7/8.6	52.9/53.6	18.0/17.6	16.3/16.7
$RbSb_2BrF_4O$	20.3/17.1	44.9/48.6	15.1/16.0	15.1/15.2
$NH_4Sb_2BrF_4O$	3.4/4.2	61.4/56.2	17.5/18.4	17.4/17.5

\* Found/calculated.

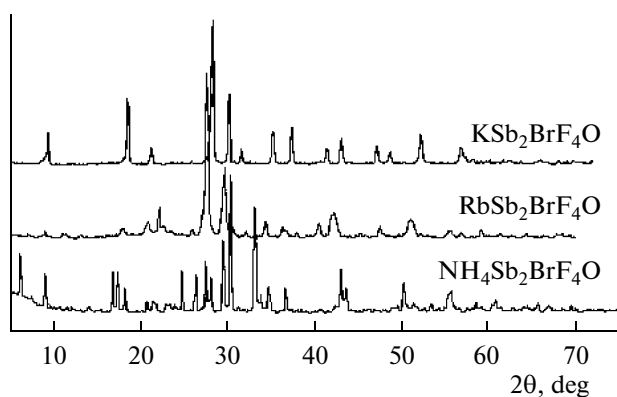


Fig. 1. Powder X-ray diffraction patterns for compounds synthesized.

range. The whiteness  $W$  and the averaged reflectance  $r$  were calculated by the standard formulas [9]:

$$W = 2R_{430} - R_{670}; \quad (1)$$

$$r = \sum_{430}^{670} R_i / 240; \quad (2)$$

where  $R$  is the reflectance.

Derivatograms were recorded on a NETZSCH STA 449C Jupiter synchronous analyzer (heating rate 5 °C/min, dry argon).  $^{19}\text{F}$  NMR spectra were recorded on a Bruker Avance AV 300 spectrometer (282.404 MHz) in the 150–500 K range. The chemical shifts  $\delta$  of the  $^{19}\text{F}$  NMR signals are referenced to  $\text{C}_6\text{F}_6$  as the external standard. The temperature setting accuracy was 2 K; the full line width at half maximum  $\Delta H$  was measured to within 1%.

## RESULTS AND DISCUSSION

Reactions of KBr, RbBr, and  $\text{NH}_4\text{Br}$  with  $\text{SbF}_3$  in aqueous solutions give poorly soluble complex oxohaloantimonates(III) of the formula  $\text{MSb}_2\text{BrF}_4\text{O}$  as described in [4]. Their X-ray powder diffraction patterns are shown in Fig. 1. We failed to characterize these complexes using single-crystal X-ray diffraction because their crystals are very small (2–15  $\mu\text{m}$  according to SEM data) [4].

### Vibrational Spectroscopy of the Complexes $\text{MSb}_2\text{BrF}_4\text{O}$ ( $M = \text{K}, \text{Rb}, \text{and } \text{NH}_4$ )

The IR spectra of fluorine- and oxygen-containing Sb(III) compounds are described in [10–13]. The characteristic feature of the IR spectra of  $\text{MSb}_2\text{BrF}_4\text{O}$  ( $M = \text{K}, \text{Rb}, \text{and } \text{NH}_4$ ) (Fig. 2a) is the absorption at 400–600  $\text{cm}^{-1}$  (Sb–F stretches) [10, 11]. The bands at 600–800  $\text{cm}^{-1}$  (Fig. 2a) are due to the Sb–O stretches. The structures of  $\text{Sb}_2\text{O}_3$ ,  $\text{Sb}_4\text{O}_5\text{Cl}_2$ , and  $\text{Sb}_3\text{O}_2\text{F}_5$ , contain bridging O atoms; the absorption bands in their IR spectra appear in the same range.

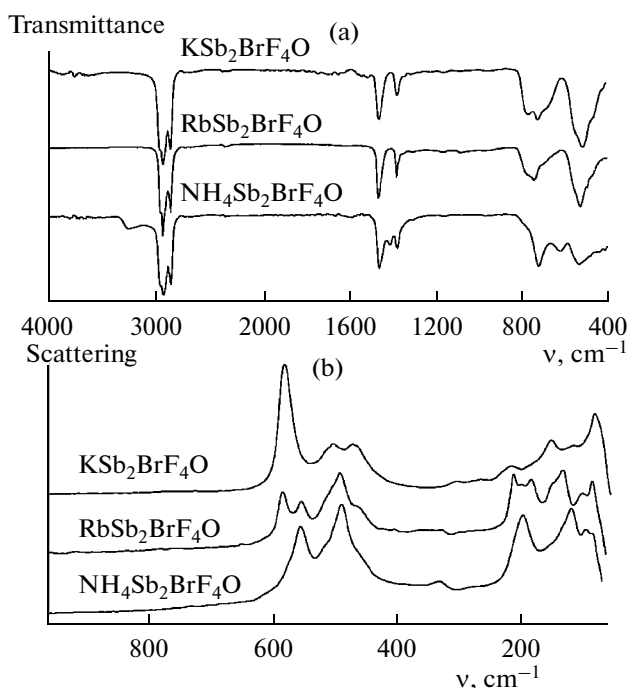


Fig. 2. (a) IR and (b) Raman spectra of compounds synthesized.

The Raman spectra of  $\text{MSb}_2\text{BrF}_4\text{O}$  (Fig. 2b) show two groups of bands at 70–220 and 450–600  $\text{cm}^{-1}$ , as in the Raman spectra of  $\text{Sb}_3\text{O}_2\text{F}_5$  in [13]. One can thus assume that the crystal lattices of the complexes  $\text{MSb}_2\text{BrF}_4\text{O}$  ( $M = \text{K}, \text{Rb}, \text{and } \text{NH}_4$ ) also contain bridging O atoms between two Sb atoms to form the groups Sb–O–Sb. The IR spectrum of  $\text{NH}_4\text{Sb}_2\text{BrF}_4\text{O}$  also exhibits absorption bands at 1410 and 3250  $\text{cm}^{-1}$  ( $\text{NH}_4^+$ ).

### Optical Properties of the Complexes $\text{MSb}_2\text{BrF}_4\text{O}$ ( $M = \text{K}, \text{Rb}, \text{and } \text{NH}_4$ )

The total reflection (R) spectra of the compounds  $\text{Sb}_3\text{O}_2\text{F}_5$ ,  $\text{Sb}_4\text{O}_5\text{Cl}_2$  (compared to a commercial sample of  $\text{Sb}_4\text{O}_5\text{Cl}_2$ ),  $\text{Sb}_8\text{O}_{11}\text{Br}_2$ , and  $\text{MSb}_2\text{BrF}_4\text{O}$  ( $M = \text{K}, \text{Rb}, \text{and } \text{NH}_4$ ) are shown in Fig. 3. The spectral patterns of all the above compounds are typical of semiconductors: a high (up to 97%) reflectance in the red region of the visible spectrum and a low (<30%) reflectance in the UV region. The spectra of simple and complex oxohalides differ mainly in the initial phase of absorption (when high reflection changes to absorption) and in the character of this change.

All the simple antimony(III) oxohalides studied begin to absorb at 330–360 nm (Fig. 3a). The reflectance, which is 74–90% in the visible region, sharply decreases to 7–30% in the UV region.

The reflectances of the complex oxohalides decrease gradually as the wavelength decreases (Fig. 3b). For  $\text{KSb}_2\text{BrF}_4\text{O}$  and  $\text{RbSb}_2\text{BrF}_4\text{O}$ , high reflection changes

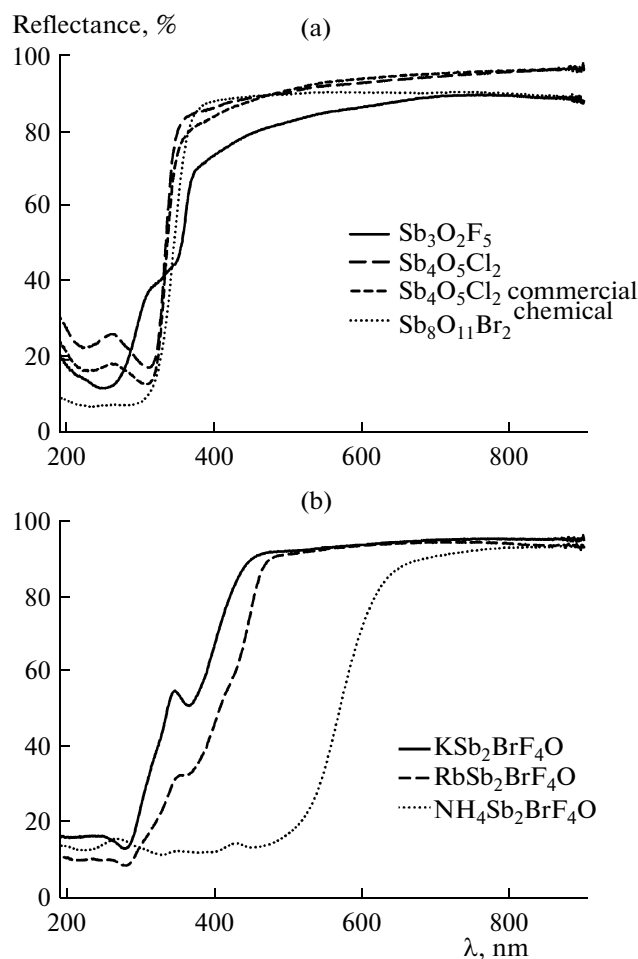


Fig. 3. (a) Optical reflectance spectra of (a) simple and (b) complex antimony(III) oxohalides.

to absorption at 450–280 nm with an intermediate peak at 350 nm, the reflectance of  $\text{RbSb}_2\text{BrF}_4\text{O}$  is lower by 10–15%. The reflectance of  $\text{NH}_4\text{Sb}_2\text{BrF}_4\text{O}$  begins to decrease at 660 nm, being as low as 12–15% at 190–460 nm.

According to the data in Table 2, the compounds  $\text{Sb}_4\text{O}_5\text{Cl}_2$ ,  $\text{Sb}_8\text{O}_{11}\text{Br}_2$ , and  $\text{KSb}_2\text{BrF}_4\text{O}$  have the highest averaged reflectances. The oxobromide  $\text{Sb}_8\text{O}_{11}\text{Br}_2$  is characterized by the highest whiteness among all the compounds studied.

#### Thermal Analysis of the Complexes $\text{MSb}_2\text{BrF}_4\text{O}$ ( $M = \text{K}, \text{Rb}, \text{and } \text{NH}_4$ )

The derivatograms of the complexes  $\text{MSb}_2\text{BrF}_4\text{O}$  ( $M = \text{K}, \text{Rb}, \text{and } \text{NH}_4$ ) are shown in Fig. 4. The complex  $\text{KSb}_2\text{BrF}_4\text{O}$  undergoes no noticeable changes over a temperature range from 25 to 230°C (Fig. 4a). On further heating, this complex melts (endothermic effect) in a range from 280 to 291°C. The weight loss to this point does not exceed 1%. Above the final melting temperature, the complex begins to decompose

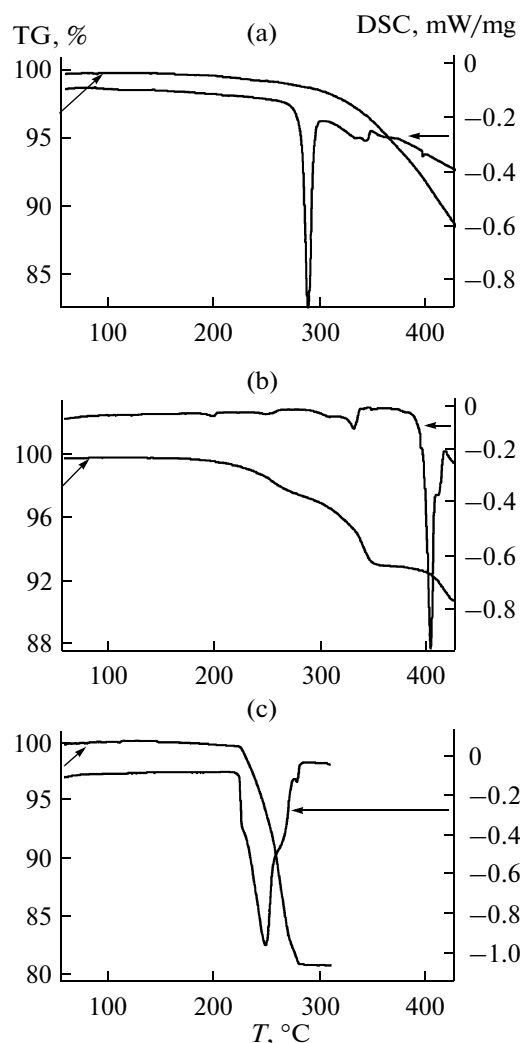


Fig. 4. Thermal curves for compounds synthesized: (a)  $\text{KSb}_2\text{BrF}_4\text{O}$ , (b)  $\text{RbSb}_2\text{BrF}_4\text{O}$ , and (c)  $\text{NH}_4\text{Sb}_2\text{BrF}_4\text{O}$ .

gradually, which is evident from several minima on the DSC curve and from gradual weight loss. The decomposition of the complex is completed at 700°C (weight loss 16.8%).

The thermolysis of  $\text{KSb}_2\text{BrF}_4\text{O}$  gives  $\text{SbF}_3$ , which evaporates above 376°C. According to X-ray powder diffraction data, IR spectra, and chemical analysis data, the residue at 700°C is a mixture of  $\text{KBr}$  and oxygen- and halogen-containing  $\text{Sb(III)}$  compounds with unidentified compositions.

The decomposition of  $\text{RbSb}_2\text{BrF}_4\text{O}$  begins at 197°C, which is evident from an endothermic effect accompanied by a weight loss (Fig. 4b). In the 200–360°C range, the complex undergoes irregular decomposition accompanied by several minima on the DSC curve and by gradual weight loss. A relatively stable phase exists at 360–400°C; on further heating, this phase melts and the complex continues to decompose.

**Table 2.** Averaged reflectance  $r$  and whiteness of antimony(III) oxohalides

Compound	$r$ , %	Whiteness, %
Sb <sub>3</sub> O <sub>2</sub> F <sub>5</sub>	85	67
Sb <sub>4</sub> O <sub>5</sub> Cl <sub>2</sub>	93	83
Sb <sub>4</sub> O <sub>5</sub> Cl <sub>2</sub> (Commercial chemical)	93	79
Sb <sub>8</sub> O <sub>11</sub> Br <sub>2</sub>	91	88
KSb <sub>2</sub> BrF <sub>4</sub> O	93	74
RbSb <sub>2</sub> BrF <sub>4</sub> O	86	—
NH <sub>4</sub> Sb <sub>2</sub> BrF <sub>4</sub> O	45	—

The complex NH<sub>4</sub>Sb<sub>2</sub>BrF<sub>4</sub>O is stable up to 223°C (Fig. 4c); further heating causes its rapid decomposition with several endothermic effects, the most pronounced minimum appearing at 247°C. The decomposition is completed at 280°C (weight loss 19.6%). The thermolysis of this complex yields Sb<sub>8</sub>O<sub>11</sub>Br<sub>2</sub> (identified by X-ray powder diffraction) as a solid residue and some gaseous products.

Thus, according to the thermal analysis data, the complexes KSb<sub>2</sub>BrF<sub>4</sub>O, RbSb<sub>2</sub>BrF<sub>4</sub>O, and NH<sub>4</sub>Sb<sub>2</sub>BrF<sub>4</sub>O are stable below 230, 197, and 223°C, respectively.

### *Ionic Mobility in Heteroleptic Antimony(III) Complexes*

To get information on the character of ionic motion in the fluoride sublattice of the complex oxohalides MSb<sub>2</sub>BrF<sub>4</sub>O (M = K, Rb, and NH<sub>4</sub>), we analyzed their <sup>19</sup>F NMR spectra (Fig. 5) in comparison with the <sup>19</sup>F NMR spectra of MSb<sub>2</sub>F<sub>7</sub> [14]. Note that the <sup>121,123</sup>Sb and <sup>79,80</sup>Br NQR spectra of these complexes show no signals at 77 K, which suggests the absence of the electric field strength gradient on the corresponding nuclei.

The <sup>19</sup>F NMR spectra of KSb<sub>2</sub>BrF<sub>4</sub>O at 150–300 K contain an asymmetric line ( $\Delta H = 43\text{--}35$  kHz) at  $\delta$  133–110 ppm with a shoulder at  $54 \pm 5$  ppm (Fig. 5a). The parameters of this line are close to those of the line in the <sup>19</sup>F NMR spectrum of KSb<sub>2</sub>F<sub>7</sub> at 300 K. The asymmetry of this line is due to the presence of non-equivalent positions of fluoride ions in the complex anion [Sb<sub>2</sub>BrF<sub>4</sub>O]<sup>−</sup> and probably to the influence of the chemical shift anisotropy (the second moments  $S_2(F)$  of the <sup>19</sup>F NMR spectra differ substantially at field strengths of 2.114 and 7.05 T). The observed spectral pattern and the high  $S_2(F)$  value below 300 K ( $\sim 27$  G<sup>2</sup>) with consideration to the NMR data for KSb<sub>2</sub>F<sub>7</sub> [14] suggests that the fluoride sublattice of KSb<sub>2</sub>BrF<sub>4</sub>O at 150–300 K remains rigid in NMR terms [15].

Above 350 K, the <sup>19</sup>F NMR spectrum of KSb<sub>2</sub>BrF<sub>4</sub>O (Fig. 5a) shows a more symmetrical “narrow” line (at 300–500 K, the line width is reduced to  $\sim 7$  kHz); the second moment decreases to  $\sim 3$  G<sup>2</sup>. In the absence of phase transitions, such spectral changes

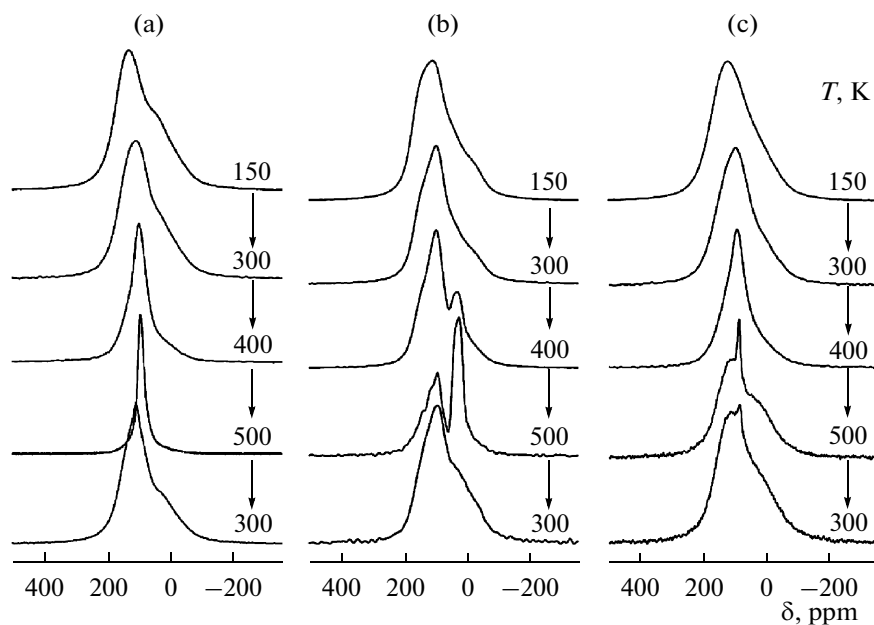


**Fig. 5.** Evolution of <sup>19</sup>F NMR spectra of (a) KSb<sub>2</sub>BrF<sub>4</sub>O, (b) RbSb<sub>2</sub>BrF<sub>4</sub>O, and (c) NH<sub>4</sub>Sb<sub>2</sub>BrF<sub>4</sub>O in response to changing temperature.

can be associated with a transformation of the rigid fluoride sublattice involving local motions. Along with the rigid sublattice, reorientations of the complex anion  $[\text{Sb}_2\text{BrF}_4\text{O}]^-$  are the most probable ionic motions at 350–450 K. The parameters of the NMR spectra (the line width and shape and the second moment) suggest high ionic mobility in the fluoride sublattice above 480 K, which can be due to partial diffusion of fluoride ions.

For a sample of  $\text{KSb}_2\text{BrF}_4\text{O}$  recooled from 500 to 300 K, the  $^{19}\text{F}$  NMR spectrum is restored only partially ( $\Delta H \approx 27$  kHz,  $\delta \approx 108$  ppm,  $S_2(\text{F}) \approx 20.5$  G<sup>2</sup>; at least, a three-component spectral pattern). Apparently, such a spectral change arises from the beginning of the decomposition of the complex.

The  $^{19}\text{F}$  NMR spectrum of  $\text{RbSb}_2\text{BrF}_4\text{O}$  at 150–200 K shows an asymmetric line at  $\delta \approx 95$  ppm ( $\Delta H = 37$ – $39$  kHz) (Fig. 5b), somewhat differing from the spectrum of the homoleptic analog  $\text{RbSb}_2\text{F}_7$  at 300 K. The asymmetry of the resonance line, as in the case of  $\text{KSb}_2\text{BrF}_4\text{O}$ , is due to the chemical shift anisotropy and the nonequivalence of the structural positions of the fluoride ions (at least three lines with different line widths and positions overlap in the spectrum). Heating from 150 to 300 K virtually does not affect the parameters of the  $^{19}\text{F}$  NMR spectrum of  $\text{RbSb}_2\text{BrF}_4\text{O}$ , which corresponds to the rigid lattice. Above 300 K, the spectral pattern changes because of a transformation of the rigid fluoride sublattice involving local motions. The  $^{19}\text{F}$  NMR spectrum exhibits a new line with a monotonically decreasing chemical shift (from  $\delta \sim 42$  to 20 ppm) and a growing intensity as the temperature is elevated. Analysis of the derivative of the  $^{19}\text{F}$  NMR spectrum in this temperature range reveals at least three components at  $\delta 145 \pm 10$  (shoulder), 97, and 42–30 ppm. Heating from 380 to 450 K causes the growth of the upfield and central components. The shoulder at  $\delta 145 \pm 10$  vanishes almost completely and the  $^{19}\text{F}$  NMR spectrum of  $\text{RbSb}_2\text{BrF}_4\text{O}$  consists of two intense lines at  $\delta 95$  and 23 ppm (Fig. 5b). Further heating causes the growth and narrowing (to  $\sim 10$  kHz) of the line at  $\delta = 25$  ppm. At the maximum experimental temperature (500 K), the peak intensity of the upfield line is higher by a factor of 1.7 than that of the line at  $\delta \approx 95$  ppm (the ratio of the line widths is  $\sim 2 : 1$ ). Analysis of the above variations in the parameters of both the lines in the  $^{19}\text{F}$  NMR spectrum (chemical shift, line width, and line intensity) with temperature, with consideration to NMR data for  $\text{RbSb}_2\text{F}_7$  [14], suggests that two forms of ionic motion can coexist in the fluoride sublattice of  $\text{RbSb}_2\text{BrF}_4\text{O}$  above 480 K. One can be associated with the reorientation of the complex anion  $[\text{Sb}_2\text{BrF}_4\text{O}]^-$  (the line at  $\delta = 95$  ppm) and the other, with the high mobility of fluoride ions (the line at  $\delta = 23$  ppm), which is attributable to the diffusion observed in the homoleptic analog  $\text{RbSb}_2\text{F}_7$  above 450 K [14]. On recoiling of the complex  $\text{RbSb}_2\text{BrF}_4\text{O}$  to ambient temperature, the  $^{19}\text{F}$  NMR spectrum virtually resumes its original shape (Fig. 5b).

The  $^{19}\text{F}$  NMR spectrum of  $\text{NH}_4\text{Sb}_2\text{BrF}_4\text{O}$  (Fig. 5c) at 150 K is similar to those of the complexes  $\text{KSb}_2\text{BrF}_4\text{O}$  and  $\text{RbSb}_2\text{BrF}_4\text{O}$ . At 300 K, the spectra of  $\text{NH}_4\text{Sb}_2\text{BrF}_4\text{O}$  and  $\text{NH}_4\text{Sb}_2\text{F}_7$  [14] are virtually identical, differing only in the line widths and positions ( $\delta = 97$  and 128 ppm, respectively). The observed spectral pattern and the line width suggest the absence of ionic motions in the fluoride sublattice with frequencies above  $10^4$  Hz.

On heating to 420 K, the line in the  $^{19}\text{F}$  NMR spectrum of  $\text{NH}_4\text{Sb}_2\text{BrF}_4\text{O}$  becomes narrowed from 36 to 17.7 kHz ( $S_2(\text{F})$  decreases from  $\sim 24$  to 15 G<sup>2</sup>). Most likely, these changes are due to local motions in the fluoride sublattice. At 420 K, the spectrum consists of two components with different intensities ( $\approx 60 : 40$ ) and different widths ( $\approx 12.5$  and 42 kHz), which are spaced apart at  $\sim 15$  ppm. Above 440 K, the spectrum shows a narrow line ( $\Delta H \approx 2.5$  kHz) with a Lorentzian profile at  $\delta \sim 90$  ppm. The spectrum becomes highly asymmetric and much wider (widening from 17.7 to 38.5 kHz); the second moment increases as well. Since this complex does not melt or decompose at this temperature, the narrow line is most likely attributable to diffusion in the fluoride sublattice. However, its area at 500 K does not exceed 4% of the total area of the  $^{19}\text{F}$  NMR spectrum, which is why local motions of fluorine-containing groups are still a dominant type of ionic mobility in the fluoride sublattice. Note that recoiling of  $^{19}\text{F}$  from 500 K to ambient temperature, the  $^{19}\text{F}$  NMR spectrum does not resume its original shape (Fig. 5c). This can be explained, as with  $\text{KSb}_2\text{BrF}_4\text{O}$ , by the decomposition of the complex which begins at 496 K (thermal analysis data).

To sum up, when moving from the homoleptic complexes  $\text{MSb}_2\text{F}_7$  ( $M = \text{K}, \text{Rb},$  and  $\text{NH}_4$ ) to the heteroleptic complexes  $\text{MSb}_2\text{BrF}_4\text{O}$ , the observed changes in the  $^{19}\text{F}$  NMR spectra are due to the changes in the dynamic processes in the fluoride sublattice, which depend on the cation  $M^+$ . On the whole, introduction of bromide and oxygen ions into the complex anion of the complexes  $\text{MSb}_2\text{F}_7$  reduces the ionic mobility in the resulting complexes  $\text{MSb}_2\text{BrF}_4\text{O}$ .

## ACKNOWLEDGMENTS

This work was supported by the Far East Branch of the Russian Academy of Sciences, project no. 09-III-V-04-123.

## REFERENCES

1. V. Ya. Kavun, N. F. Uvarov, A. B. Slobodyuk, et al., *Russ. J. Electrochem.* **41**, 488 (2005).
2. L. A. Zemnukhova and R. L. Davidovich, *J. Fluorine Chem.* **45**, 71 (1989).
3. L. A. Zemnukhova and R. L. Davidovich, *Koord. Khim.* **8**, 1572 (1982).

4. A. E. Panasenko, L. A. Zemnukhova, and K. N. Galkin, *Vest. Dalnevost. Otd. Ross. Akad. Nauk*, No. 2, 125 (2009).
5. R. L. Davidovich and L. A. Zemnukhova, *Koord. Khim.* **1** (4), 477 (1975).
6. Kiseleva, E.K., *Analysis of Fluorine-Containing Compounds* (Khimiya, Moscow, 1966).
7. W. J. Williams, *Handbook of Anion Determination* (Butterworth-Heinemann, 1979; Khimiya, Moscow, 1982).
8. *Chemical Encyclopedia*, Ed. by I. L. Knunyants (Sovetskaya entsiklopediya, Moscow, 1988), Vol. 1 [in Russian].
9. E. F. Belen'kii and I. V. Riskin, *Chemistry and Technology of Pigments* (Khimiya, Leningrad, 1974) [in Russian].
10. R. L. Davidovich, T. A. Kaidalova, T. F. Levchishina, et al., *Collection of Infrared Absorption Spectra and X-ray Diffraction Data on Fluorides of Group IV and V Elements* (Nauka, Moscow, 1972) [in Russian].
11. N. M. Laptash, E. V. Kovaleva, A. A. Mashkovskii, et al., *Zh. Strukt. Khim.* **48** (5), 907 (2007).
12. K. I. Petrov, Yu. M. Golovin, and V. V. Fomichev, *Zh. Neorg. Khim.* **18**, 2922 (1973).
13. E. I. Voit, A. E. Panasenko, and L. A. Zemnukhova, *Zh. Strukt. Khim.* **50**, 66 (2009).
14. V. Ya. Kavun and V. I. Sergienko, *Diffusion Mobility and Ion Transport in Crystalline and Amorphous Fluorides of Group IV Elements and Antimony(III)* (Dal'nauka, Vladivostok, 2004) [in Russian].
15. A. G. Lundin and E. I. Fedin, *NMR Spectroscopy* (Nauka, Moscow, 1986) [in Russian].